

Vibration based Health Monitoring and Damage Diagnosis of Al-Alloy 7075 T6 Beam Structure

Edukrishnan.V
M. Tech: Mechanical Department
NCERC Pampady
Thrissur

Manuraj K R
Assistant Professor
Mechanical Department
NCERC Pampady

Eldho Jacob Joy
Assistant Professor
PSG Engineering College
Coimbatore

Abstract:- This paper describes about the numerical and experimental analysis of Al Alloy 7075 T6 beam structure. The frequency changes are obtained and Proceeded for further calculations. The experimental analysis is done with the help of vibration analyzer equipment and specimens are created for the experimental evaluation. Timoshenko beam theory was used as base theory. Both numerical and experimental models were analyzed and validated with help of Ansys and VMAP software.

I. INTRODUCTION

With a tremendous growth in the past years, structural health monitoring (SHM) has emerged as a well-recognized field of technology. The essential concerns of structural Health monitoring involve the integration of smart materials such as sensors, data processing, modern computational power and decision making algorithms into structures to detect damage and access the integrity to predict the remaining lifetime based on projected loading and environmental conditions. Regular non-destructive evaluation (NDE) techniques such as liquid penetrant, magnetic particles, radiography, Ultrasonics and eddy current methods often require off-line inspection and the knowledge of possible damaged areas. The inaccessibility to the inspection location could result in great challenges and even become prohibitive for most NDE techniques. Structural health monitoring, on the other hand, may have an array of sensors attached on or imbedded in the host structure in service, and be able to continuously monitor in real time, those physical parameters that can be further processed for damage detection and health status assessment. This inaccessibility issues could be eliminated to the lowest possible level. The downtime for pre scheduled maintenance as well as associated costs is greatly reduced.

II. THEORY

A Timoshenko beam theory:

The Timoshenko beam theory which was developed by Stephen Timoshenko early in the 20th century. The model takes into account of shear deformation and rotational bending effects, making it suitable for describing the behaviour of short beams, sandwich composite beams which subject to high-frequency excitation when the wavelength approaches the thickness of the beam. The resulting equation is 4th order but, unlike ordinary Euler-Bernoulli beam theory, there is also a second-order partial derivative present.

Taking into account the added mechanisms of deformation effectively lowers the stiffness of the beam, while the result is very large deflection under a static load and lower predicted eigen frequencies for a set of boundary conditions. The latter effect is more noticeable for higher frequencies as the wavelength becomes shorter, and the distance between opposing shear forces decreases.

If the shear modulus of the beam material reaches infinity - and the beam becomes rigid in shear - and if rotational inertia effects neglected, then Timoshenko beam theory converges towards ordinary beam theory.

B Aim of health monitoring of structures:

Above all, SHM has great amount of aspirations that, if achievable, would hugely benefit society at large. Further to this, the aim is that, after detection, any defect could be located and its severity inferred so that decisions can be easily made to what actions needed to be taken next. These global objectives for SHM have been well formalized in Rytter's hierarchy, which classifies these aims into 'levels' of increasing difficulty as follows:

Level 1 (DETECTION): The method shows a qualitative indication that damage might be present in the structure.

Level 2 (LOCALISATION): The method Shows information about the probable position of the damage.

Level 3 (ASSESSMENT): The method gives an estimate of the range of the damage.

Level 4 (PREDICTION): The method offers information about the safety of the structure, e.g. predicts a residual life.

Although it has number of changes and additions to this hierarchy have been suggested in the literature,

Level 1 (DETECTION): The method gives a qualitative indication that damage might be present in the structure.

Level 2 (LOCALISATION): The method showed information near the probable position of the damage.

Level 3 (CLASSIFICATION): The method offer information about the type of damage.

Level 4 (ASSESSMENT): The method gives an estimate of the extent of the damage.

Level 5 (PREDICTION): The method offers information about the safety of the structure.

Material properties

Aluminium has many benefits over other materials, including a high strength to weight ratio, corrosion resistance, formability, and price. Alloy 2014, 7075, 2219 and 2024 are engineered to be lightweight and strong, and their ease of formability allows complex shapes and drawn parts, which can then be further enhanced with heat treating. Mostly used non-ferrous metallic materials are Aluminium alloys. Use of these alloys reduces the weight of the systems considerably.

Properties

- Higher strength to weight ratio
- Resistance to corrosion by many chemicals
- High thermal and electrical conductivity
- Non-toxicity and reflectivity
- Ease of formability and machinability & Non-magnetic

Designation

The principal alloying elements in Aluminium alloys are; Copper, Manganese, Silicon, Magnesium and Zinc. The alloys are identified by four digit numbers of the form of "Nxxx" where the value of 'N' denotes, the major alloying elements.

- 1xxx = Commercially pure Aluminium
- 2xxx = Copper
- 3xxx = Manganese
- 4xxx = Silicon
- 5xxx = Magnesium
- 6xxx = Magnesium and Silicon
- 7xxx = Zinc

The second digit shows alloy modification .If the second digit is zero. It indicates the original alloy: digits 1 through 9, which are assigned progressively, indicate alloy modifications.

Aluminium Alloy 7075-T6

This is of the highest strength aluminium alloys available. Its strength to weight ratio is excellent and it is ideally used for highly stressed parts. It is formed in the annealed condition and subsequently heat treated. Spot or flash welding is used, although arc and gas welding are not recommended. It is available in the clad ("Alclad") form to enhance the corrosion resistance with the total strength being only moderately affected. Applications: Used where highest strength is needed.

General Group

Aluminium Alloy AA 7000 Series (Aluminium-Zinc Wrought Alloy)

General Form

7075 (AlZn5.5MgCu, 3.4365, 2L95, A97075) Aluminium

Material Properties

- Density : 2.80 g/cm³ (175 lb/ft³)
- Elastic (Young's, Tensile) Modulus : 72 GPa (10 x 106 psi)
- Electrical Conductivity : 33 % IACS
- Elongation at Break : 11 %

- Fatigue Strength (Endurance Limit): 160 MPa (18 x 103 psi)
- Melting Onset (Solidus) : 477 °C (891 °F)
- Shear Modulus : 27 GPa (3.9 *106 psi)
- Shear Strength : 331MPa (48 x 103 psi)
- Specific Heat Capacity : 960 J/kg-K
- Strength to Weight Ratio : 211 kN-m/kg
- Tensile Strength: Ultimate (UTS) : 590 MPa
- Tensile Strength: Yield (Proof) : 510 MPa
- Thermal Conductivity : 130 W/m-K
- Thermal Diffusivity : 48
- Thermal Expansion : 23.2 µm/m-K

II METHODOLOGY AND PROCEDURES

Convergence test

A fundamental theory of using the finite element procedure is that the body is sub divided up into small discreet regions known as finite elements. These elements stated by nodes and interpolation functions. Governing equations are written for each element and those elements are assembled into a global matrix. Loads and constraints are applied and the solution is then determined. But the problem is regarding the accuracy of the solution. It must be found out, to trust the solution how far or how small the element must be divided. It will be necessary to conduct convergence tests for these. By these it means that we analyze with a mesh discretization and then observe and record the solution. The problem is repeated with finer mesh (i.e. more elements) and then compared with the results of the previous tests. If the results are nearly similar, then the first mesh is good enough for that particular geometry, loading and constraints. If the results differ by a huge amount however, it will be necessary to try a finer mesh yet. Finer meshes come with however: more calculation time and large memory requirements. It is desired to find the minimum number of elements that gives the converge solution.

Table 1: Results of convergence testing

Mesh Division	First Natural Frequency (Hz)	Second Natural Frequency (Hz)	Third Natural Frequency (Hz)
2	1.4593	8.5637	9.6238
3	1.4521	8.5526	9.1948
4	1.4489	8.5533	9.1024
5	1.4472	8.5542	9.0711
6	1.4463	8.5552	9.0575
7	1.4457	8.5563	9.0505
8	1.4453	8.5569	9.0466
9	1.4451	8.5571	9.0443
10	1.4449	8.5570	9.0426
11	1.4448	8.5569	9.0414
12	1.4446	8.5567	9.0404
13	1.4445	8.5566	9.0395
14	1.4445	8.5566	9.0395

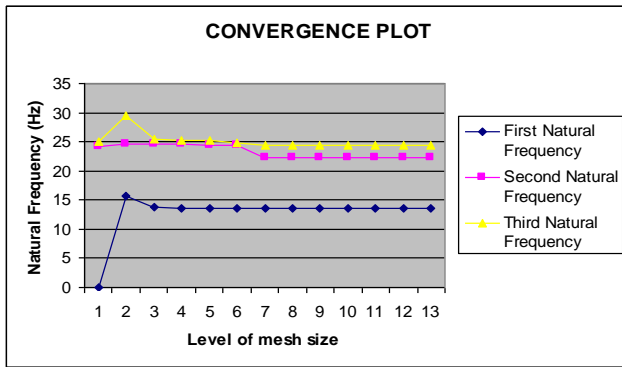


Fig 1: Convergence plot

IV VIBRATION ANALYSIS

Introduction

After carrying out the convergence study of the non-cracked beam various crack situations are simulated using the ANSYS 15.0 CAE software package. The results of the non-dimensional natural frequencies as a function of various crack locations are presented here. Initially the cracks are simulated for a uniform crack depth of 0.1 at various crack locations. The locations are indicated in terms of relative crack locations from the fixed end. The beam is made up of Aluminium alloy 7075-T6 material.

The geometrical characteristics of the beam are taken as length = 300mm, breadth = 30mm and height = 10mm respectively. The finite elements were taken as brick 8 Node 45. These were selected because, due to the presence of cracks, the beam will assume an irregular cross section. The material properties were as listed in table.

The crack locations and crack depths were varied to obtain the vibration characteristic of the beam. So, the variables are Relative Crack Location (RCL) and the Relative Crack depths (RCD)

$$RCL = \frac{\text{Length of the beam at crack}}{\text{Original Length}}$$

$$RCD = \frac{\text{Depth of the crack (a)}}{\text{Height of the beam (h)}}$$

Six RCL values were taken by keeping each RCD constant. The various relative locations were taken at 0.1, 0.2, 0.4, 0.6, 0.8, and 0.9 respectively. The presented method has been applied for free vibration analysis of a non-cracked and cracked aluminium alloy cantilever beam. Free vibration analysis of a cantilever cracked aluminium alloy beam has been examined by using finite element method (FEM). Throughout this investigation, the element type was selected as Hex. In addition to this, meshing was swept and the smart size was selected as two. The boundary conditions were applied and the model was solved. The method for solving was Block lanczos.

The entire process is classified into two parts

- I. Numerical analysis
- II. Experimental analysis

In numerical analysis section vibration analysis is carried out in Ansys APDL 15.0. Variation of natural frequency on account of location and variation of natural frequency on account of depth had calculated. The entire specimen is divided into 9 parts and set of frequencies have been found out. Graph has been plotted for each case. In the experimental analysis Al-Alloy 7075 specimen is analyzed with help of vibration analyzing device. Cracked specimen and Healthy specimen are produced. Crack has been generated with the help of slitting saw. Accelerometer, data acquisition device, VMAP software.etc are parts of the experimental device. The specimen is fixed in a vibration isolator table and accelerometer is fixed at various positions and with the help of a hammer the specimen is excited and these creates vibration which is absorbed by data acquisition device and it is transformed to VMAP software which is operated using a computer. Set of frequencies are derived from the information absorbed. The graph which validates the finite element analysis and Experimental modal analysis is plotted.

A. Numerical analysis

Variation of natural frequency on account Of location

In the first six runs the beam having a constant relative crack depth (RCD) = 0.1 is simulated at various locations i.e. at 0.1, 0.2, 0.4, 0.6, 0.8 and 0.9 were analyzed and the following values were obtained.

Table 2: Natural frequencies at various crack locations at RCD of 0.1

RCL	First Natural Frequency	Second natural Frequency	Third natural frequency
0.1	1.4373	8.5384	9.0168
0.2	1.4390	8.5423	9.0306
0.3	1.4404	8.5455	9.0271
0.4	1.4415	8.5482	9.0162
0.5	1.4423	8.5503	9.0085
0.6	1.4429	8.5519	9.0096
0.7	1.4433	8.5533	9.0174
0.8	1.4436	8.5546	9.0260
0.9	1.4438	8.5559	9.0316

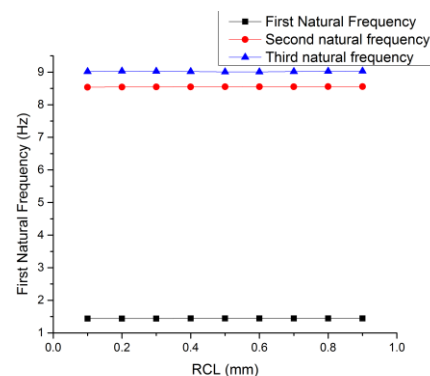


Fig 2: Relative Crack location versus Natural Frequencies at RCD = 0.1

Table 3: Natural frequencies at various crack locations at RCD of 0.6

RCL	First Natural Frequency	Second natural frequency	Third natural Frequency
0.1	1.2237	7.9732	8.5923
0.2	1.2776	8.1303	9.0227
0.3	1.3268	8.2652	8.8444
0.4	1.3689	8.3747	8.3841
0.5	1.4019	8.0899	8.4569
0.6	1.4247	8.1194	8.5130
0.7	1.4382	8.4327	8.5472
0.8	1.4447	8.5661	8.8198
0.9	1.4474	8.5770	9.0210

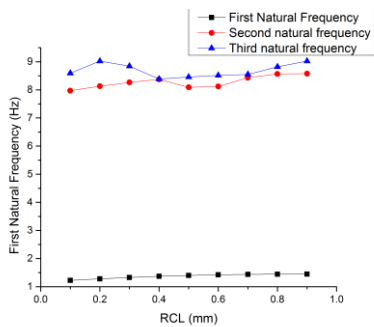


Fig 3: Relative Crack location versus Natural Frequencies at RCD = 0.1

RCL	First Natural Frequency	Second natural Frequency	Third natural frequency
0.1	0.8041	7.2899	8.0614
0.2	0.9015	7.6011	9.0033
0.3	1.0103	7.8841	8.4148
0.4	1.1268	7.0579	8.1259
0.5	1.2420	6.2117	8.3153
0.6	1.3404	6.0385	8.4472
0.7	1.4067	6.5874	8.5264
0.8	1.4385	7.8758	8.5665
0.9	1.4483	8.5851	8.9278

Table 4: Natural frequencies at various crack locations at RCD of 0.8

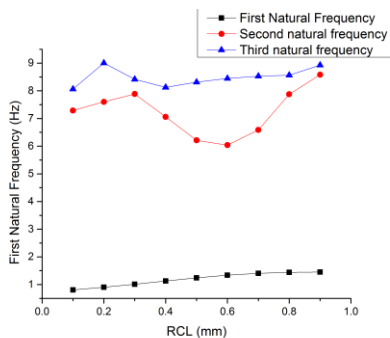


Fig 4: Relative Crack location versus Natural Frequencies at RCD = 0.1

RCL	First Natural Frequency	Second natural frequency	Third natural frequency
0.1	0.3868	6.7247	7.7950
0.2	0.4548	7.1368	8.9860
0.3	0.5430	7.5298	8.0188
0.4	0.6597	5.9732	7.8820
0.5	0.8151	4.6411	8.1697
0.6	1.0163	3.9627	8.3764
0.7	1.2393	3.9246	8.5016
0.8	1.3966	5.0131	8.5631
0.9	1.4462	8.2384	8.5887

Table 5: Natural frequencies at various crack locations at RCD of 0.8

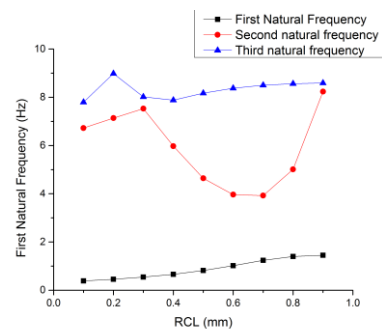


Fig 5: Relative Crack location versus Natural Frequencies at RCD = 0.1

Variation of natural frequency on account of depth

By rearranging the above results we can find the vibration characteristics of the beam (Variation of natural frequencies) at a specific location for example, In the first six runs the beam is having a crack at location 0.1 (constant RCL = 0.1). However the depth of the crack varies from 0.1 to 0.9. This crack growth is analyzed and the following results were noted. In the next six runs the beam having a constant relative crack length (RCL) = 0.1 is simulated at various locations i.e. at 0.1, 0.2, 0.4, 0.6, 0.8 and 0.9 and were analyzed and the following values were noted.

Table 6: Natural frequencies at various crack locations at RCD of 0.8

RCD	First Natural Frequency	Second natural Frequency	Third natural frequency
0.1	1.4373	8.5384	9.0168
0.2	1.4247	8.5051	8.9882
0.3	1.4031	8.4425	8.9396
0.4	1.3692	8.3422	8.8669
0.5	1.3137	8.1889	8.7552
0.6	1.2237	7.9732	8.5923
0.7	1.0655	7.6762	8.3529
0.8	0.80411	7.2899	8.0614
0.9	0.38689	6.7247	7.795

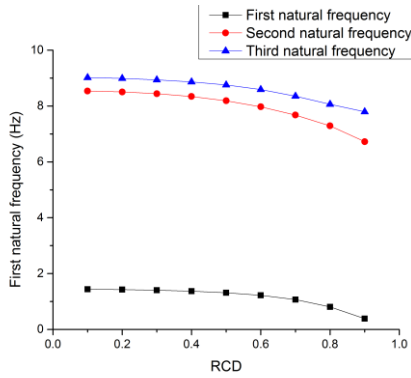


Fig 6: Relative Crack location versus Natural Frequencies at RCD = 0.1

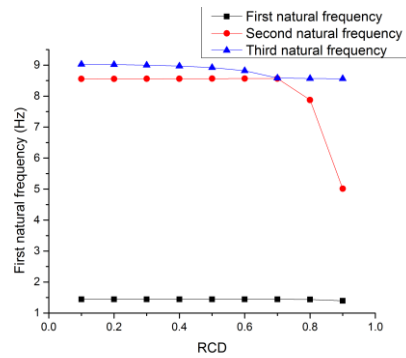


Fig 8: Relative Crack location versus Natural Frequencies at RCD = 0.1

Table 7: Natural frequencies at various crack locations at RCD of 0.8

Table 9: Natural frequencies at various crack locations at RCD of 0.8

RCD	First Natural Frequency	Second natural Frequency	Third natural frequency
0.1	1.4429	8.5519	9.0096
0.2	1.4422	8.5508	8.9624
0.3	1.4408	8.5473	8.8783
0.4	1.4383	8.541	8.7429
0.5	1.4337	8.5128	8.5300
0.6	1.4247	8.1194	8.5130
0.7	1.4033	7.3757	8.4866
0.8	1.3404	6.0385	8.4472
0.9	1.0163	3.9627	8.3764

RCD	First Natural Frequency	Second natural frequency	Third natural frequency
0.1	1.4438	8.5559	9.0316
0.2	1.4446	8.5603	9.0326
0.3	1.4453	8.5644	9.0326
0.4	1.4460	8.5687	9.0318
0.5	1.4467	8.5728	9.0285
0.6	1.4474	8.5770	9.0210
0.7	1.4480	8.5811	8.9998
0.8	1.4483	8.5851	8.9278
0.9	1.4462	8.2384	8.5887

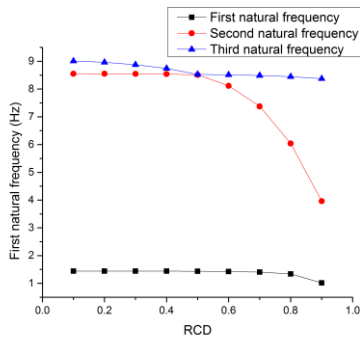


Fig 7: Relative Crack location versus Natural Frequencies at RCD = 0.1

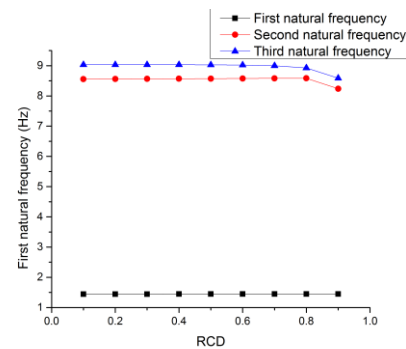


Fig 9: Relative Crack location versus Natural Frequencies at RCD = 0.1

Table 8: Natural frequencies at various crack locations at RCD of 0.8

RCD	First Natural Frequency	Second natural Frequency	Third natural frequency
0.1	1.4436	8.5546	9.0260
0.2	1.4440	8.5575	9.0165
0.3	1.4444	8.5601	8.9992
0.4	1.4447	8.5626	8.9708
0.5	1.4449	8.5645	8.9190
0.6	1.4447	8.5661	8.8198
0.7	1.4434	8.5668	8.5819
0.8	1.4385	7.8758	8.5665
0.9	1.3966	5.0131	8.5631

The graphs plotted between the first, second and the third natural frequencies with the relative crack locations and the depths clearly indicate the variation of natural frequencies according to the position and the depth of the crack.

On account of position as the crack moves from the fixed end to the free end it is found that initially the frequencies rise and become maximum at an RCL of 0.6 and further the frequency decreases. This variation is almost same for the case of second and third natural frequencies. The beam exhibits the same characteristics for uniform crack depth of 0.1 and 0.2. In the case of beam with uniform crack depth of 0.4, the natural frequencies tend to rise towards the free end of the beam and attain a maximum value at an RCL of 0.9.

But in the case of beam with crack of uniform crack depth of 0.6 the natural frequencies becomes maximum at RCL 0.4 and then it is found to decrease towards the free end of the beam. Finally in the case of uniform crack depth of 0.8 and 0.9, the natural frequency tends to decrease in the middle of the beam. The frequencies are highest in the fixed as well as the free end of the beam.

This is the general variation of the natural frequency of the beam due to the presence of a crack of uniform depth along the length of the beam. Thus the crack growth at a particular location can be identified if the beam exhibits similar characteristics as that of given above provided the geometrical characteristics as well as the material properties remains the same.

B. Experimental analysis

Specimen preparation

Aluminium alloy 7075 T-6 beam with dimensions 300mm X 30 mm X 10mm has to be made. Nine equal parts have to be made. One healthy and eight cracked specimens are proposed to be analysed. The specimen is to be divided into nine equal parts at first. Water jet machining is used for this purpose. Then crack have to be made on Eight equal parts this is done by Slitting saw in milling machine. The specimen is then ready for experimental analysis.



Fig10: Specimen for vibration analysis

Vibration analyzer

VMAP is a complete software tool for vibration testing on real-world engineering systems that seamlessly connects virtual simulation and physical testing.

Vibration Measurement and Analysis Package (VMAP) represents the convergence of virtual prototype and prototype testing. There are several parameters that cannot be modeled accurately in existing virtual prototyping tools which are dependent on experimental methods. VMAP bridges this gap between virtual prototyping and experimentation in design cycle especially in the development of automotive, aerospace and energy systems. The system significantly improves productivity of product design team by not only cutting costs and development time but also intangibles associated with mistakes in design.

VMAP is a versatile software platform powered by accurate and predominant algorithm, friendly user-interfaces, rich and fast graphics and supports industry-standard file formats.

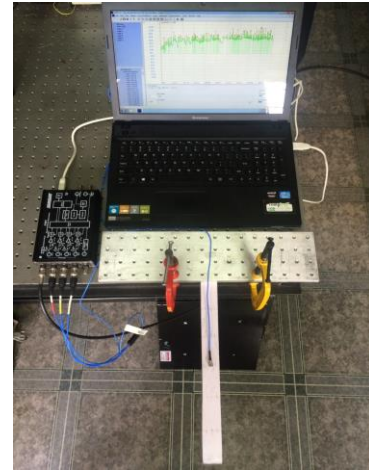


Fig 11: Vibration analyzer equipment

Validation of experimental modal analysis and finite element analysis

The validation of the experimental and modal analysis is done for the accuracy of the analysis. The relative crack length is plotted with respect to various crack depth. The accuracy is determined according to comparison of these values. VMAP software is used for the validation.

V map software

VMAP or Vibration Measurement and Analysis Package developed by Tech Passion Technologies, is an experimental modal analysis and finite element validation software. It enables you to do vibration studies of machines and structures by performing data acquisition, modal parameter estimation and correlation between test and FE data on a unified platform thus bridging the gap between virtual prototyping and testing.

- Data Acquisition and Measurement System
- Experimental Modal Analysis
- FE Correlation and Validation

Components

- Geometry creation and import module that allows you to either create wireframe geometry in VMAP or import ANSYS, NASTRAN and .STL mesh geometry. You can also import modal analysis results from both experiment and simulation.
- Data acquisition system to acquire vibration signatures from sensors mounted on different points on the test specimen. Single Input, Single Output (SISO), and the Single Input, Multiple Output (SIMO) configurations are supported for hammer and shaker excitations.
- Analysis module that enables you to plot and view time and frequency domain signals, frequency response functions and post-process them to extract modal parameters such as accurate natural frequencies and damping ratios of the component.

FE-test correlation_tool to visually and quantitatively correlate mode shapes obtained from both experiment and simulation for the same test component.

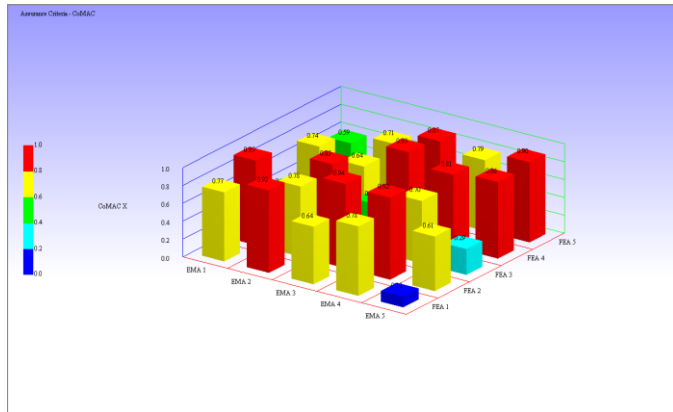


Fig 12: Validation result of FEA and EMA

V. DISCUSSION

The above results show the validation of Finite element analysis and experimental modal analysis of Al-alloy 7075 T6 beam. The results while observed clearly state that the finite element analysis and Experimental modal analysis was highly accurate. The values which is in red color or the graph bar which is in red color is highly accurate because the value is near to 1. If the value is 1 then the test is 100 percent successful, in practical cases 100 percent efficiency is not achievable. So if a near value to 1 makes the validation successful. The Modal Assurance Criterion (MAC) matrix is a mathematical tool to compare two vectors to each other. It can be used to investigate the validity of estimated modes. The MAC between two mode shape vectors $\{\psi\}_r$ and $\{\psi\}_s$ is defined as,

$$MAC(\{\Psi\}_r, \{\Psi\}_s) = \frac{(\{\Psi\}_r^{*T} \{\Psi\}_s)^2}{(\{\Psi\}_r^{*T} \{\Psi\}_r) (\{\Psi\}_s^{*T} \{\Psi\}_s)}$$

The MAC will approach the value 1 if $\{\psi\}_r$ and $\{\psi\}_s$ are the same mode shape. If $\{\psi\}_r$ and $\{\psi\}_s$ are different mode shapes, the MAC value should be low, due to the orthogonality condition of the mode shapes.

VI. CONCLUSION

From the investigations it can be concluded that the natural frequencies of vibration of a cracked Al-alloy beam are the functions of the crack locations and crack depths. The presence of a transverse crack increases the natural frequencies of the Al-alloy beam. On account of position as the crack moves from the fixed end to the free end it is found that initially the frequencies rise and become maximum at an RCL of 0.6 and further the frequency decreases.

In the case of beam with uniform crack depth of 0.4, the natural frequencies tend to rise towards the free end of the beam and attain a maximum value at an RCL of 0.9. But in the case of beam with crack of uniform crack depth of 0.6 the natural frequency becomes maximum at RCL 0.4 and then it is found to decrease towards the free end of the beam. In the case of uniform crack depths of 0.8 and 0.9, the natural frequency tends to decrease in the middle of the beam. The frequencies are highest in the fixed as well as the free end of the beam.

VII. REFERENCES

- [1] Vinay V. Kuppast, Vijay Kumar N. Chalwa, S. N. Kurbet, Aravind M. Yadawad(2014).Finite element analysis of aluminium alloys for their vibration characteristics. IJRET: International Journal of Research in Engineering and Technology eISSN: 2319-1163 pISSN: 2321-7308.
- [2] Eldho Jacob joy and Dr. Biju N, Analysis of cracked composite cantilever beam, December 2014.
- [3] Jasim M. Salman (2013). Improvement Properties of 7075-T6 Aluminum Alloy by Quenching in 30% Polyethylene Glycol and Addition 0.1%B. ISSN 2320-6055.
- [4] H.R.Chiranjeeve, K.Kalaichelvan, A.Rajadurai(2014). DESIGN and VIBRATION ANALYSIS of a 2U-CUBESAT STRUCTURE USING AA-6061 for AUNSAT – II. e- ISSN: 2278-1684, p-ISSN : 2320-334X.
- [5] G.M Sayeed Ahmed, Sirajuddin Elyas Khany, Syed Hamza Shareef(2014). Design, Fabrication and Analysis of a Connecting Rod with Aluminum Alloys and Carbon Fiber. Vol. 3, Issue 10, October 2014, ISSN: 2319-8753.